Werk

Jahr: 1970
Kollektion: fid.geo
Signatur: 8 Z NAT 2148:36
Digitalisiert: Niedersächsische Staats- und Universitätsbibliothek Göttingen
Werk Id: PPN101433392X_0036
PURL: http://resolver.sub.uni-goettingen.de/purl?PPN101433392X_0036

LOG Id: LOG_0137
LOG Titel: Observations with synchronously-offset beams on a 77 km path at 1.8 and 4 cm
LOG Typ: article

Übergeordnetes Werk

Werk Id: PPN101433392X
PURL: http://resolver.sub.uni-goettingen.de/purl?PPN101433392X

Contact

Niedersächsische Staats- und Universitätsbibliothek Göttingen
Georg-August-Universität Göttingen
Platz der Göttinger Sieben 1
37073 Göttingen
Germany
Email: gdz@sub.uni-goettingen.de

Zeitschrift für Geophysik, 1970, Band 36, Seite 621—642. Physica-Verlag, Würzburg

Observations with Synchronously-Offset Beams on a 77 km Path at 1.8 and 4 cm

By H. JESKE[1]), H. D. SEEHARS[2]), G. PUCHER[1]), H. CASSEBAUM[2]), Hamburg

Eingegangen am 13. Juni 1970

Summary: The offset beam technique proves to be a promising indirect meteorological method to investigate the space-time variant troposphere. The results are gained on the basis of the tropospheric scatter theory. A displacement of the scattering volume in vertical direction (change of scattering angle, cf. experiment A) gives information about the shape of the spatial refractive-index spectra, displacements in the direction transmitter — receiver and orthogonal to it permit statements on homogeneity and isotropy of the medium (cf. experiments B, C). This paper gives first results of our experiments with scaled antenna systems of 7 GHz and 16 GHz on a 77.2 km transhorizon path over sea. For the wave number range of the refractive-index structure between 10 and 40 m^{-1} the offset beam fieldstrength data show practically no difference from the theory of homogeneous and isotropic turbulence. The difficulties of our investigations exist in the fact that the influence of the maritime surface duct on propagation has to be separated from the tropospheric scatter field component. Thus the observations may only be interpreted in aspects of scatter propagation during poor propagation conditions (vanishing duct) and remarkable vertical antenna elevations ($\alpha > 2°$).

Some results fading of the analysis are shown too (e. g. correlations between fading rate and fading depth on the one hand, and wind velocity, median field strength, and scattering angle on the other hand).

Zusammenfassung: Die Antennen-Schwenk-Technik ist eine vielversprechende indirekte meteorologische Methode zur Untersuchung der raum-zeitlichen Struktur der Atmosphäre. Die Ergebnisse erhält man auf der Basis der troposphärischen Streutheorie, wonach der Streuanteil des Empfangsfeldes und seine Veränderlichkeit (Fading) von der Struktur des Brechungsindexfeldes und des Windfeldes im gemeinsamen Volumen abhängen. Die Verlagerung des streuenden Volumens in vertikaler Richtung (Änderung des Streuwinkels) gestattet Aussagen über die Form des BI-Spektrums (Exp. A), Verlagerungen längs des Ausbreitungsweges und quer dazu geben Aufschlüsse über Homogenität und Isotropie des Mediums (Exp. B, C). Die hier diskutierten Experimente wurden mit Hilfe schwenkbarer Antennensysteme auf einer Überhorizontstrecke zwischen Bremerhaven und Helgoland gleichzeitig auf den Frequenzen 7 GHz und 16,5 GHz durchgeführt. Die Arbeit gibt erste Resultate. Für den Wellenzahlbereich der BI-Struktur zwischen 10 und 40 m^{-1} zeigte sich, daß das Spektrum der BI-Fluktuationen im Mittel den theoretisch bei homogener und isotroper Turbulenz erwarteten entspricht. Besondere Schwierigkeiten auf der relativ kurzen Meßstrecke stellte die Separation des Ducteinflusses dar. Unter dem Aspekt der reinen Streuausbreitung konnten so nur Beobachtungen bei verschwindender Ductdicke und gleichzeitig merklicher Anhebung der Antennen ($\alpha > 2°$) betrachtet werden.

Einige Ergebnisse der Fadinganalyse (u. a. Korrelationen der Fadingrate und der Fadingtiefe einerseits mit dem Wind, der Medianfeldstärke und dem Streuwinkel andererseits) werden ebenfalls mitgeteilt.

[1]) Meteorologisches Institut der Universität Hamburg.

[2]) Institut für Radiometeorologie und Maritime Meteorologie an der Universität Hamburg (Institut der Fraunhofer-Gesellschaft).

1. Introduction

A variety of different indirect measurements of atmospheric structure have been derived from troposcatter signal observations obtained with antenna beams directed off the great circle propagation path [e. g.: CRAWFORD et al.; 1959; GJESSING, 1962; KOONO et al., 1962; BIRKEMEIER et al., 1968]. During 1967 and 1968 three extended radiometeorological experiments with offset beams were conducted by the University of Hamburg[1], [2]). The measuring area was a 77.2 km path over the German Bight between the island Heligoland and Bremerhaven, Germany. Two frequencies, 6. 8 and 16.5 GHz, were transmitted and received by adjacent parabolic antennas situated at each terminal on the coast at about 30 m above mean sea level. A "common" volume was obtained by the use of antennas of 1,8° half-beam width for *both* frequencies. On standard refraction conditions (4/3 earth) the receiver was located within the diffraction zone (about 30 km beyond the total radio horizon).

The radiometeorological observations discussed in this paper were made in a variety of weather conditions. We used them to examine the applicability of indirect methods on shorter transhorizon links, especially to isolate the effects of the lower maritime surface layer—which frequently gives rise to duct propagation. The signal amplitude, long-period fieldstrength and short-period fading, were used for an estimation of the shape (power law) of the atmospheric refractivity spectrum, the homogeneity and isotropy of the turbulent refractivity field, and some characteristics of the wind field.

2. Theoretical Background

2.1. *Propagation in the Space Variant Atmospheric Medium*

A measure of the intensity of scattered radiation is—provided that the Born approximation is applicable—the scattering cross-section σ, defined as the energy scattered into the direction of $\vec{k}_2$, per unit volume, per unit solid angle, per unit incident power density. On condition of statistical homogeneity, the scattering cross section (σ) and scattered power (P_s) resp., is given by [e. g. TATARSKI, 1961]

$$P_s \sim \sigma = 2\pi k_1^4 \cdot \sin^2 \chi \cdot \Phi(\vec{K}), \tag{1}$$

where χ is the depolarization angle between the incident electric field vector $\vec{k}_1$ and the propagation vector $\vec{k}_2$ (χ usually 90°) and $\Phi(\vec{K})$ the 3-dimensional refractive index spectrum.

The wave number vector $\vec{K}$ results from the vector difference between the wave number vector $\vec{k}_1$ of the incident field and that one of the scattered field ($\vec{k}_2$).

[1]) Meteorologisches Institut der Universität Hamburg and the

[2]) Institut für Radiometeorologie und Maritime Meteorologie an der Universität Hamburg (Institut der Fraunhofer-Gesellschaft).

$$\vec{K}=\vec{k}_1-\vec{k}_2\,,\quad k_1=k_2=2\pi/\lambda\,, \tag{2}$$

(λ: wave lenght of radiation).

Provided that the antenna heights are identical, $\vec{K}$ is directed vertically. The magnitude of $\vec{K}$ is given by

$$K=2k(\sin\Theta/2)=(4\pi/\lambda)(\sin\Theta/2)\,, \tag{2a}$$

(Θ: scattering angle, see fig. 1).

The linear extensions of refractive index inhomogeneities which contribute mainly to the power density of the receiver are

$$L(\Theta)=\lambda/(2(\sin\Theta/2))\,. \tag{2b}$$

During the offset beam experiments the position of the scattering volume is considerably shifted in space, a fact which involves statistical non-homogeneity, that is to say σ is a function of position (x, y, z). Taking into consideration variations of the

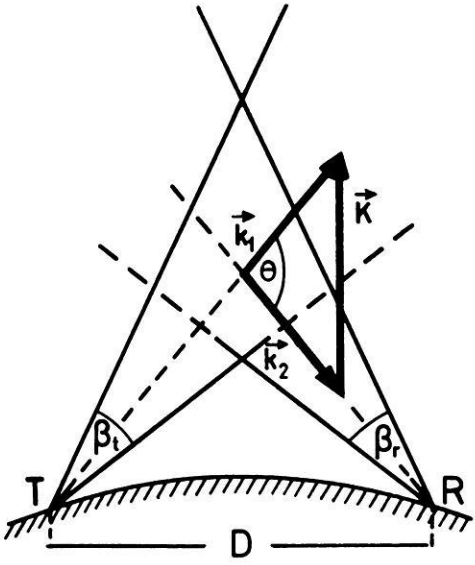

Fig. 1: Geometry of a troposcatter path

R = receiver, T = transmitter, D = distance $T-R$, $\vec{k}_1$, $\vec{k}_2$ = wavenumber vector components of the incident (into the scattering volume) wave and the wave scattered into the direction of receiver. $\vec{K}$ = spectral component of the three-dimensional refractive index wavenumber spectrum. Θ = scattering angle, $\beta_t=\beta_r$: half beam width of transmitting and receiving antennas, resp.

scattering cross-section with spatial position, GJESSING [1964] uses as a first approximation the following equation:

$$\sigma \sim \nu(x, y, z) \cdot \Phi(\vec{K}). \tag{1a}$$

In this way ν is a criterion for the lack of homogeneity with regard to variations of the scattering volume in space.

For the spectrum of the refractive index field one may write [TATARSKI, 1961]:

$$\Phi|(\vec{K})| = \Phi(2k \sin \Theta/2) \sim K^{-n} \sim (2k \sin \Theta/2)^{-n} \sim ((4\pi/\lambda) \sin \Theta/2)^{-n}. \tag{3}$$

Then one may succeed in determining the exponent (n) of refractive index spectrum from the angular *and* wave length dependence of fieldstrength (E). It is easy to show with the help of (1) and (3) that the following equations are valid for both the methods ($E^2 \sim p_s$):

$$\left(\frac{E_{\Theta_{i+1}}}{E_{\Theta_i}}\right)^2 = \frac{V_{i+1}}{V_i} \left(\frac{\sin \Theta_{i/2}}{\sin \Theta_{i+1/2}}\right)^n \tag{4}$$

E_{Θ_i}, $E_{\Theta_{i+1}}$ are the scattered field strengths, V_i, V_{i+1} the scattering volumes, which correspond to the scattering angles Θ_i and Θ_{i+1}, resp.:

$$\left(\frac{E_1}{E_2}\right)^2 = \left(\frac{E_{01}}{E_{02}}\right)^2 \cdot \left(\frac{\lambda_1}{\lambda_2}\right)^{n-4} \tag{5}$$

E_1, E_2: received fieldstrengths, E_{01}, E_{02}: free space fieldstrengths, which correspond to wave lengths λ_1 and λ_2. Note that E_{01} and E_{02} contain the cable power losses of the transmitter and receiver set up.

Table 1 gives the exponent n and the wave length dependence δ ($\delta = n - 4$) according to different authors. Values 1—4) are based upon scattering theories (homogeneous and isotropic structures), values 5—7) upon theories of diffuse reflection (inhomogeneous structures for which formulas similar to (1) may be derived —with $\Phi(\vec{K}, \vec{R}_2)$ instead of $\Phi(\vec{K})$; $\vec{R}_2$: vector distance scatterer-receiver).

Table 1: The wave number dependence of refractive index spectrum (n) and the corresponding wave length dependence (δ) of scattered power according to some well known theories.

			n	δ
1)	Megaw-Obukhov	[Megaw 1950]	3.67	−1/3
2)	Villars-Weisskopf	[1954]	4.33	1/3
3)	Villars-Weisskopf	[1955]	5	1
4)	Booker-Gordon	[1950]	4	0
5)	Du Castel et al.	[1960]	5 to 6	1 to 2
6)	Eklund	[1968]	4 to 8	0 to 4
7)	Friis et al.	[1957]	4.8	4/5

2.2. *Analysis of Offset Beam Experiments*

The interdependence of $\Phi(\vec{K})$ and the received power (1) involves that the variation of $\vec{K}$ leads to variations of the received power. Observed variations of received power as a function of $\vec{K}$ give therefore results with respect to $\Phi(\vec{K})$. In order to prove the validity of the concept of homogeneity and isotropy one only need to determine the variations of refractive index spectrum $\Phi(\vec{K})$ in space. In this way the following offset beam experiments were carried out (corresponding to GJESSING's [1962, 1969] experiments):

Experiment A consists in the displacement of the somewhat changing scattering volume in vertical direction above the mid-path point (s. fig. 2) by simultaneous vertical elevation of both the antennas. In this experiment the magnitude of the wave number vector $\vec{K}$ changes because of the variation of Θ, whereas the direction of $\vec{K}$ remains constant. According to formula (1), it is possible to determine the

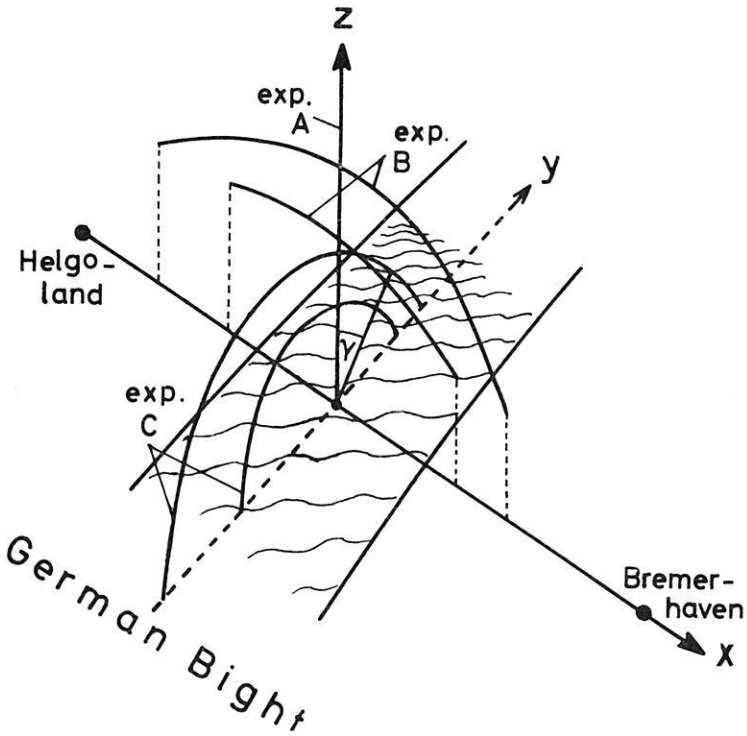

Fig. 2: Schematic three-dimensional diagram of position of the scattering volume for vertical (exp. A) and azimuthal (exp. C) antenna elongations and for those along the connection line transmitter — receiver (exp. B).

refractive index spectrum from the variation of the mean fieldstrength as a function of the scattering angle. Particularly the shape of the refractive index spectrum (the exponent n) may be calculated by the aid of equ. (4).

Experiment B consists in the displacement of the scattering volume into the direction of the connection line of the transmitting and receiving antennas (s. fig. 2 and dotted line in fig. 3). This experiment corresponds to experiment A), but note that on the one side the antenna elevation is increased, while on the other side it is decreased simultaneously by the same angle. The scattering angle and thus $|\vec{K}|$ remain exactly constant, the direction of $\vec{K}$ is changed by some 6° in the maximum.

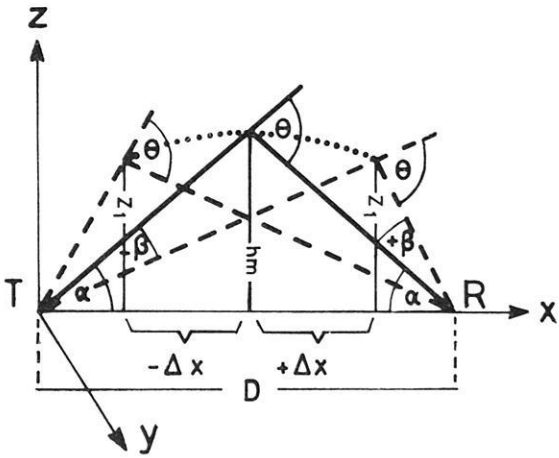

Fig. 3: Diagramm of the antenna elevations in experiment B. The following geometrical points accord with following adjustments of the antenna:

$P(D/2, h_m)$	antenna elevation	$\alpha_t = \alpha_r = \alpha$
$P((D/2) - \Delta x, z_1)$	antenna elevation	$\alpha_t = \alpha + \beta; \alpha_r = \alpha - \beta$
$P((D/2) + \Delta x, z_1)$	antenna elevation	$\alpha_t = \alpha - \beta; \alpha_r = \alpha + \beta$

Note that beside the displacement into the direction of transmitter and receiver, resp., (dir. x) the scattering volume is shifted vertically (dir. z). To test the degree of homogeneity ($\nu(x)$) only the positions of the scattering volume can be compared, which are shifted to either side of the mid-path-position (symmetrical positions). The comparison of mid-path-position and asymmetrical positions of scattering volume (difference in altitude between both the positions) leads to results with respect to $\nu(z)$, provided that the degree of homogeneity in x-direction is known. $\nu(z)$ may be used for a correction of the effect of non-homogeneity in experiment A).

Experiment C consists in the synchronous rotation of the antennas with the scattering volume (exactly constant in this experiment). The antennas describe a circular arc in the plane perpendicular to the connection line of transmitter and receiver above mid-path-position. Note that this experiment can be carried out for different radii of the circular arc—corresponding to different vertical antenna elevations. In this case the scattering angle Θ and $|\vec{K}|$ remain constant, while the direction of $\vec{K}$ changes (by variation of the angle γ). The variations in the wave number spectrum of refractive index is a function of orientation of the vector $\vec{K}$ in space. This experiment gives information about the degree of isotropy of atmospheric turbulence, provided that it is legitimate to attach the vector $\vec{K}_{\gamma=45°}$ to the vector $\vec{K}_{\gamma=0°}$. Note, however, that one has to take account of the effects of non-homogeneity following from the displacements of the common volume into y- and z-direction ($v(y, z)$. $v(z)$ and $v(x)$ are derived from experiment B), $v(y)$ is assumed to have the same order of magnitude as $v(x)$.

2.3. *Variation of Geometry During Offset Beam Experiments*

The calculation of the geometrical data was carried out by the use of the general ray equation:

$$\frac{d}{dx}\left(\frac{dz}{dx}\right)+f(z)\cdot\left(\frac{dz}{dx}\right)^2-g(z)=0. \tag{7}$$

$f(z)$ and $g(z)$ are dependent on the modified refractive index gradient, z and x are the coordinates directed vertically and in the connection line transmitter—receiver resp. dz/dx corresponds to the angle of the wave path to the horizontal. The refractive index was assumed to be a linear function of height (refractive index gradient: $-0.4\cdot10^{-7}$/m and $-0{,}7\cdot10^{-7}$/m respectively). In this case the differential equation can be integrated. From the variation of the angle of elevation (angle of the wave path to the horizontal) follow the geometric parameters given in table 2.

Table 2a contains scattering angle (Θ), size (L) of the scattering inhomogeneities and the corresponding wave numbers (K), height (h_m) of the centre of common volume above mid-path-point, size (y) of the scattering volume, and vertical extension (h_v) of the volume as function of vertical antenna elevation angle (experiment A).

Considering the volumes calculated, one has to take into account the fact that for small vertical antenna elevations the lower part of the antenna lobes is screened off by the earth curvature.

The geometrical data calculated show that our experiments may be valid for heights up to about 2.8 km and for wave numbers up to 20 m^{-1} and 50 m^{-1} (7 and 16 GHz) resp.

Table 2b contains the horizontal displacement ($2\cdot\Delta x$) and heights h (Δx) of the scattering volume as a function of antenna elevation angle α_t and α_r resp. (experiment B), s. fig. 3) and the azimuthal displacement Δy and corresponding heights h_γ of scattering volumes as function of angle γ (experiment C).

Table 2a: Geometrical parameters for experiment A*).

α	Θ	L (7 GHz)	L (16 GHz)	K (7 GHz)	K (16 GHz)	h_m	V	h_v
[°]	[m rad]	[m]	[m]	[m^{-1}]	[m^{-1}]	[m]	[km^3]	[m]
0	3.7 (1.7)	11.9	4.9	0.50	1.3	14 (4.6)	1.138	606
0.5	21.2 (19.2)	2.1	0.9	2.9	6.1	353 (330)	1.835	943
1.0	38.7 (36.6)	1.2	0.5	5.2	12.6	690 (667)	2.153	1213
1.5	56.1 (54.0)	0.8	0.3	7.8	21.0	1027 (1003)	2.098	1234
2.0	73.5 (71.4)	0.6	0.25	10.5	25.0	1364 (1340)	2.040	1264
2.5	90.0 (87.8)	0.5	0.2	12.5	31.4	1702 (1679)	1.980	1313
3.0	108.5 (106.3)	0.4	0.17	15.7	36.9	2039 (2015)	1.910	1358
3.5	125.9 (123.6)	0.35	0.15	18.0	41.8	2377 (2352)	1.820	1407
4.0	143.4 (141.0)	0.30	0.12	20.9	52.3	2716 (2692)	1.700	1461

*) Scattering angle (Θ), size (L) of the scattering inhomogeneities and the corresponding wave numbers (K), height (h_m) of the centre of common volume above the mid-path point, size (V) of the scattering volume, and vertical extension (h_v) of the volume as function of vertical antenna elevation angle α (experiment A). Assumption: Linear refractive index gradient of $-0.4 \cdot 10^{-7}$/m and $-0.7 \cdot 10^{-7}$/m (in brackets).

Table 2b: Geometrical parameters for experiments B and C*).

α_t/α_r	$2 \cdot \Delta x$	$h(\Delta x)$	$\Delta y_\gamma = 15$	$\Delta y_\gamma = 30$	$\Delta y_\gamma = 45$	$h_\gamma = 15$	$h_\gamma = 30$	$h_\gamma = 45$
[°]	[km]	[m]	[m]	[m]	[m]	[m]	[m]	[m]
1/1	—	690	178	345	488	667	599	488
2/2	—	1364	253	632	956	1238	1171	956
3/3	—	2039	528	1019	1442	1970	1766	1442
1.5/0.5	34.9	356						
3/1	36.7	1039			no measurements			
4/2	24.9	1821						

*) Horizontal displacement ($2 \cdot \Delta x$) and heights $h(\Delta x)$ of the scattering volume as a function of antenna elevation angle α_t and α_r, resp. (experiment B, see fig. 3) and the azimuthal displacement Δy and corresponding heights h_γ of scattering volumes as function of angle γ (experiment C).

2.4. *Propagation in the Time Variant Atmospheric Medium*

Temporal variations of the refractive index field cause the signal fading of the receiving fieldstrength. In the case of scatter propagation moving scattering elements give rise to a Doppler shift of the frequency of an electromagnetic wave. Most of the fading theories use the "single-scatterer" concept, requiring a linear relationship between the Doppler spread on the one hand, and normal path horizontal component of the wind velocity and scattering angle on the other hand. In this way GJESSING [1962] suggests for the width of the Doppler spectrum:

$$\Delta f = 2/\lambda \cdot (v \sin \beta + \Delta v(\gamma) \sin \Theta/2), \tag{6}$$

where v: cross-path-component of mean wind velocity, β: beam-width, $\Delta v(\gamma)$: fluctuating component of the wind into the direction of γ ($\approx 90°$ for experiment A), Θ: scattering angle, λ: wave length. On the basis of equ. (6), we are able to gain informations about the mean and the turbulent wind field, if the fading rate (which is proportional to the Doppler spread) is known. Note, however, that the assumption of "single scatterer'$_t$ concept becomes already doubtful in the case of extended scattering volumes [s. BIRKEMEIER et al., 1968].

Some short remarks should be made with respect to the amplitude of signal fading. The theory of Rice-distribution [s. NORTON et al., 1955] characterizes the "fine structure" of signal amplitudes, which is formed by the superposition of a constant (here mostly duct influence) and a rms-component (influence of scattering) of fieldstrength. The contribution of both components to the received field may in any case be determined according to this theory if the median value and the fading depth are known. Note, that the general Rice-distribution is limited by the normal distribution (dominating constant component) on the one hand, and the Rayleigh distribution (pure scattering) on the other hand.

3. Experimental Procedures

3.1. *Radio Measurements*

It ought to be sufficient to make only some short statements on the experimental procedures. The power outputs of the 7 GHz- and 16 GHz-transmitters were 25 and 10 W CW, resp. We used parabolic antennas with an aerial gain of 38 dB. The 7 GHz receiving set up was charakterized by a minimum detectable signal level of -115 dBm and the dynamic range was 80 dB. The corresponding values of 16 GHz were -130 dBm and 90 dB (for $\alpha > 2$ the noise level of the systems often was reached). Unlike the 7 GHz-receiver the 16 GHz-receiver yielded a considerable attenuation of the amplitudes for signal fluctuations > 1 Hz (effect of smaller band width).

The synchronous rotation of the antennas (see chap. 2.2.) was performed with the help of stepping motors, the control system was an electronic one. A wireless transmission system enabled the antenna elevation to be changed simultaneously or indi-

vidually by steps of 0.5° as well vertically as azimuthally. The accuracy of adjustment was better than 0.05°.

The data were stored on analog magnetic tapes; ink recorders for control were at hand. A second 7 GHz link (somewhat changed carrier frequency) was used for the determination of the variations of the mean fieldstrength level during the offset beam experiments.

Generally the fieldstrength was recorded during 2—3 min for each orientation of the antennas. The analogue data were digitalized by the use of a scanning frequency of 60 Hz on a CDC 1700 computer, and for each antenna elevation mean values, variances, cumulative distributions, fading rates, autocorrelation functions, a. s. o. were determined. Up to now a fading analysis was carried through for 7 GHz only, because the amplitude attenuation of the rapid fluctuations on 16 GHz requires special precautions.

3.2. *Meteorological Observations*

The following meteorological program was carried out during the offset beam experiments:

a) hourly meteorological routine measurements on light house ship Elbe 1 (which is situated in mid-path position) for the determination of the refractive index stratification inside the lower maritime boundary layer. From this one will succeed in determining the thickness z^* of evaporation duct [BROCKS, 1955; JESKE, 1965] which plays an important role for the prediction of UHF- and SHF-propagation conditions above sea;

b) radiosonde ascents and radar wind measurements at Heligoland to investigate the vertical temperature-, humidity-, and wind-stratification up to heights of some km.

Note that all meteorological observations in the considered area collected by the meteorological stations of the German Weather Service at Heligoland, Bremerhaven, and Cuxhaven could be used, especially the measurements of rain gauges (evaluation of absorption effects).

4. Interpretation

4.1. *Influence of the Lower Maritime Surface Layer*

UHF and SHF propagation on short transhorizon paths above the sea is essentially influenced by the evaporation duct [JESKE, 1965; JESKE and BROCKS, 1966], which is caused by evaporation and turbulent mixing processes inside the maritime surface layer. In 80% of time a strong correlation between the receiving fieldstrength and the thickness of the evaporation duct is observed (variations between O and 20 m, yearly average 5—7 m) according to the duct theory [e. g. BOOKER-WALKINSHAW, 1946]. This effect is connected with an intensive scintillation fading, which may be interpreted as a superposition of a constant component (duct) and a rms-component (scattering).

Stable propagation conditions produced by strong advection ducts or elevated layers were observed in 20% of time. Such cases could be eliminated during the experiments in question by the aid of radiosonde ascents (chapt. 3.2.) and the consideration of the special fading characteristics.

Fig. 4 gives examples of the vertical experiments, comprising the difference of fieldstrength $\Delta F_\alpha = F_0 - F_\alpha$ (F_0, F_α observed fieldstrengths at antenna elevations $\alpha = 0$ and α fixed) as a function of α (experiment A). To show the influence of the evaporation duct, the path antenna gain loss deduced from the antenna characteristics is presented (extracted and dashed thin curves in fig. 4a, b, c). A discussion of the decrease of the fieldstrength difference ΔF_α as a function of elevation is trivial, but note that this decrease is much more intensive on 7 GHz than on 16 GHz. The influence of the evaporation duct thickness z^* can obviously be recognized as well by fig. 4a (individual example) as by fig. 4b and c (all observations for the given intervals of duct thickness). On both frequencies the increase of fieldstrength difference is considerably smaller for vanishing duct thickness ($z^* \leq 2$ m) than in the presence of a duct ($7 \leq z^* \leq 8$ m). Observed values of 16 GHz are generally smaller than those expected from the antenna pattern. During duct situations the values observed on 7 GHz are always *below*, for vanishing duct, however, very often *above* the antenna pattern. It has to be suggested that during duct conditions the propagation on 7 GHz is characterized by an additional tropospheric attenuation, even for smaller vertical antenna elevations (fig. 4b). This effect on the 7 GHz link is well known from eralier

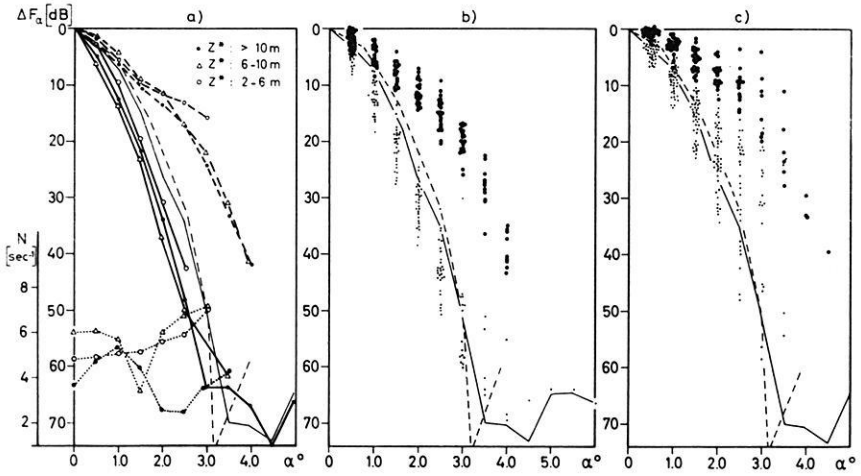

Fig. 4: Fieldstrength received for 16 and 7 GHz(ΔF_α) and fading rate (N) for 7 GHz(N, s. left part) as a function of the vertical antenna-elevation α (scattering angle $\Theta \approx 2\alpha$). Left figure: individual examples; central figure: 8 m $\leq z^* \leq$ 7 m; right figure: $z^* \leq$ 2 m.

investigations with quasi-horizontal radiating antennas, when the observed field-strengths were considerably smaller than those deduced from duct theory [JESKE and BROCKS, 1966]. The attenuation may be explained by turbulent scattering of the energy within the duct and by scattering at the rough sea surface and the rough upper boundary of the duct. On the other hand an additional tropospheric space ray component may be almost always attributed to 16 GHz propagation and, in the case of vanishing duct thickness, to 7 GHz propagation too. This points to a tropospheric scattering effect especially dominant for elevation angles $> 2°$ (fig. 4c).

Fig. 5 illustrates the facts discussed and shows the influence of the absolute field-strength level, containing the correlation diagrams for the fieldstrength of antenna elevations of $\alpha = 1°$ and $\alpha = 3°$, resp. versus the fieldstrength for quasi-horizontal radiation ($\alpha = 0$). The dependence expected from the path antenna gain is given by the broken lines. Obviously the additional scattering component becomes more

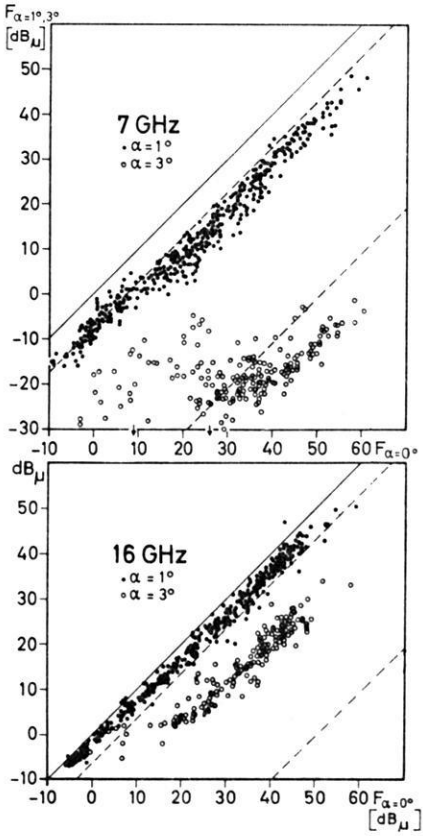

Fig. 5: Simultaneous fieldstrength received F_α [dB$_\mu$] for different antenna elevation angles.

intensive during poor propagation conditions. At $\alpha = 3°$ all 16 GHz observations are more than about 35 dB above the expected values (i. e. a pure scatter field is present), and for 7 GHz 50% of the data are now more than 10 dB above the expected values (i. e. the scatter component dominates, s. chap. 4.4.).

In order to interprete the observations in view of scatter propagation, the results mentioned above suggest that pure scattering can only be expected in the case of vanishing duct thickness ($z^* \leq 2$) and antenna elevations $> 2°$.

4.2. *Estimation of the Atmospheric Refractivity Spectrum*

Angular Dependence of Fieldstrength

Using the observations of experiment A), the determination of the shape of the refractive index spectrum (exponent n) is carried out on the basis of equ. (4). The resultant cumulative distribution is given in fig. 6 for angle variations from 1° to 1,5°, 1.5° to 2°, 2° to 2.5°, 2.5° to 3°. The corresponding distributions for both frequencies differ from each other but slightly. With increasing elevation angle the distributions are shifted towards grater n-values. The distributions following from the fieldstrength variations between $\alpha = 2°$ and $\alpha = 2.5°$, and between $\alpha = 2.5°$ and $\alpha = 3°$ show but small differences. Obviously the distributions tend towards a limiting value confirming the preponderance of one definite mechanism (for both frequencies). Assuming the distribution of an α-variation from 2.5° to 3° as the representative one the median value of n for 16 GHz amounts to 3.6 and for 7 GHz to 3.7, i. e. there exists a good correspondence to the isotropic turbulence theory of KOLMOGOROFF-HEISENBERG-OBUKHOV, which gives an exponent of 3.66. If we take into account only cases with a duct thickness smaller than 4 m (30 cases for 7 GHz and 40 cases for 16 GHz) the exponent n reduces to 3.58 (16 GHz) and 3.62 (7 GHz).

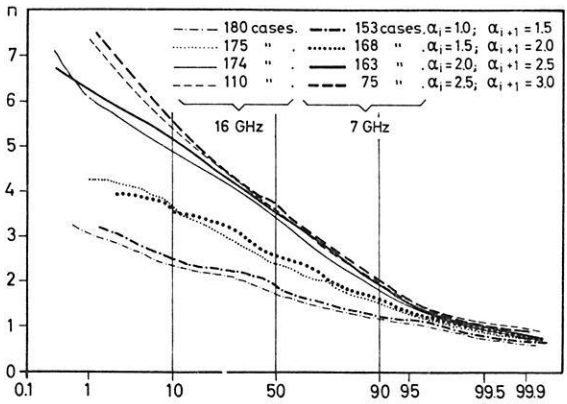

Fig. 6: Comulative distribution of the exponent n of the refractive index spectra ($\Phi(K) \sim K^{-n}$) derived from the angular dependence of fieldstrength.

As the scattering on the 16 GHz-path is caused by blobs with a diameter of 0.2 m and the scattering on the 7 GHz-path by blobs with a diameter of 0.5 m (s. table 2a) the correspondence to the theory of isotropic turbulence is more understandable. Even from the results of direct measurements we are disposed to assume isotropic values for smaller blobs [GOSSARD, 1960]. In 10% of all cases values of $n = 5.6$ and 2 respectively are found on the 7 GHz-link and values of $n = 5.4$ and 1.9 respectively on the 16 GHz-link.

An analysis of the curve following from the antenna diagrams gives n-values of 1.98 or 1.95 (on 7 GHz or 16 GHz) for a variation of α from 1° to 1.5°, 2.75 or 2.70 for α from 1.5° to 2°, 4.1 or 4.0 for α from 2° to 2.5°, and 5.2 or 5.3 for α from 2.5° to 3°. These values show that the influence of the antenna diagram is limited to smaller antenna elevations.

Wavelength Dependence of Fieldstrength

This second method to determine the exponent n arises from equ. (5). The correspondent cumulative distribution of n is given in fig. 7. A systematic shift of the curves in the direction of smaller (negative) n-values is to be seen as a function of the elevation angle. At $\alpha = 2°$, 2.5°, and 3° the distributions are almost identical and show nearly no difference in the median value. If we consider the distribution at $\alpha = 2.5°$ as the representative one there is a median value of the exponent n of 2.6, i. e. an essentially smaller value than that one obtained from the Θ-dependence (within the same α-range). For scatter propagation both methods should yield the same n-value. The discrepancy remains even if cases with a duct thickness < 4 m only are taken into account although the exponent increases to $n = 3$ (at $\alpha = 2.5°$), to 2.92 (at $\alpha = 2°$), and to 2.92 (at $\alpha = 3°$) resp.

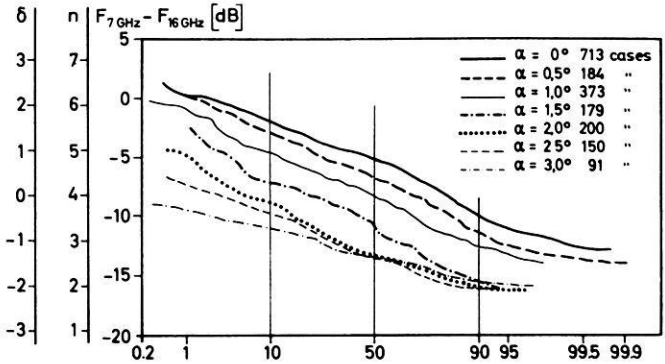

Fig. 7: Cumulative distribution of the exponent n of the refractive index spectra ($\Phi(K) \sim K^{-n}$) derived from the wave length dependence ($\lambda^{+\delta}$) of fieldstrength (7 and 16 GHz).

Note, however, that absorption influences the propagation on 16 GHz. On the link considered water vapour attenuation (including a little oxygen effect) is always effective and leads to an attenuation of 1.5 to 3 dB, which is an additional one with respect to the 7 GHz-link. Assuming a distance containing clouds and fog of 10 km, the attenuation increases once more by about 2—4 dB, i. e. we may take altogether account of an additional attenuation of 4 to 6 dB on 16 GHz. This fact leads to an increase of 1.04 to 1.56 for the exponent n corresponding to $n = 3.64$ and 4.1. The exponents derived from the two methods then approach essentially each other.

The determination of n from the wave length dependence, however, is uncertain in our case, because the absorption effects on 16 GHz can only be roughly evaluated.

The exponents n deduced from the Θ-dependence remain correct (even for 16 GHz), for the absorption effects compensate each other since the lengths of both the paths (for $\alpha = 2^\circ$ and $\alpha = 2.5^\circ$) differ but slightly (20 m).

In spite of the restriction mentioned above, the observed effects (for $\alpha > 2^\circ$) may on an average be explained by pure scatter propagation. It should be pointed to the theories of diffuse reflection which assume remarkably higher exponens than $n = 3.66$ under plausible meteorological conditions.

4.3. *Estimation of the Homogeneity and Isotropy of the Turbulent Refractivity Field*

Test of Homogeneity (Exp. B)

A survey of the effects resulting from experiment B) is given in fig. 8a and 8b. Fig. 8a gives informations about the homogeneity function in x-direction ($v(x)$). It shows the (absolute) fieldstrength levels of both frequencies for extreme displacements of the scattering volume in x-direction obtained by antenna elevation angles of $\alpha_t = 1.5^\circ/\alpha_r = 0.5^\circ$ (α_t and α_r denote the elevation angles of transmitting and receiving antenna resp.) versus the fieldstrength obtained by $\alpha_t = 0.5^\circ/\alpha_r = 1.5^\circ$, and the measurements for the adjustments $\alpha_t = 1^\circ/\alpha_r = 3^\circ$ versus $\alpha_t = 3^\circ/\alpha_r = 1^\circ$, and $\alpha_t = 4^\circ/\alpha_r = 2^\circ$ versus $\alpha_t = 2^\circ/\alpha_r = 4^\circ$. These situations correspond to displacements in x-direction (s. table 2b) of 35 km, 37 km, and 25 km, resp. On an average the differences of fieldstrength amount to 0 dB for 7 GHz with a standard deviation of ± 2.3 dB and to 0.1 dB for 16 GHz with a standard deviation of ± 1.6 dB; a systematic deviation cannot be ascertained. Therefore, in the fine-scale structure of the refractive index field in x-direction we may largely assume homogeneity, somewhat more marked for 16 GHz than for 7 GHz. Note that these results are perhaps superimposed by temporal variations of the fieldstrengths which cannot be exactly eliminated in each case.

Even if the fieldstrengths of the symmetrical adjustments ($\alpha_t = \alpha_r$) are compared with those of the unsymmetrical adjustments (s. fig. 8b), i. e. if the homogeneity in z-direction is considered ($v(z)$), larger systematic differences are not to be found. A change of the adjustments of the antennas from $\alpha_t = \alpha_r = 2^\circ$ to $\alpha_t = 3^\circ/\alpha_r = 1^\circ$ (lower part of fig. 8b) yields a displacement of the scattering volume from 1340 m

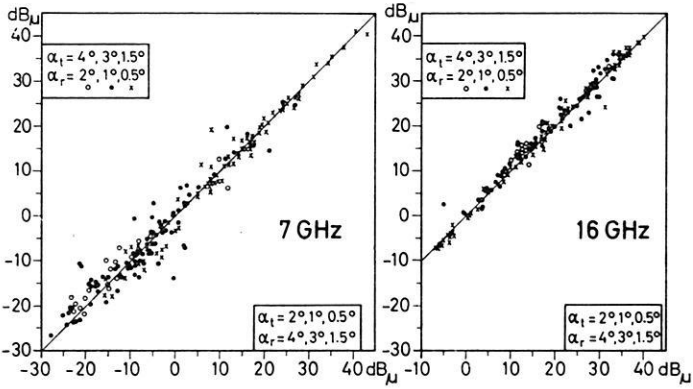

Fig. 8a: Simultaneous fieldstrength received for different antenna elevation angles (homogeneity experiment).

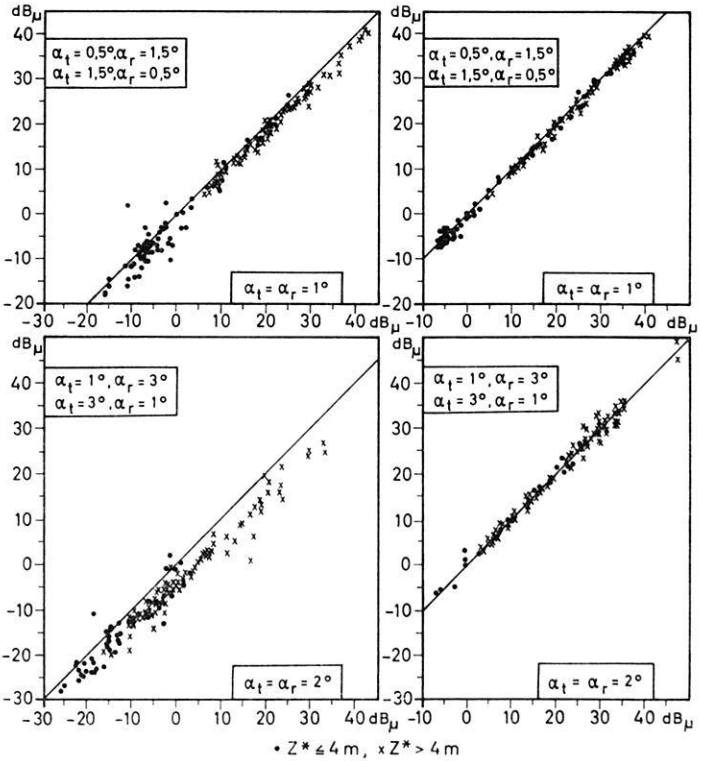

Fig. 8b: Simultaneous fieldstrength received for different antenna elevation angles

($\alpha_t, \alpha_r = \alpha + \beta, \alpha - \beta$, resp. $\rightarrow \alpha_t = \alpha_r = \alpha$, s. fig. 3)
(homogeneity experiment);
● $z^* \leq 4$ m, × $z^* > 4$ m.

to 1040 m (s. table 2b). If for 7 GHz one only takes account of situations with a duct thickness <4 m, a height effect of about 1 dB/100 m may be deduced as a first approximation. For 16 GHz such an effect is not observed. A consideration of this effect would decrease the n-values of 7 GHz derived from the Θ-dependence of fieldstrength by 0.15, i. e. to $n = 3.55$ for $\alpha = 2.5°$ what means that the median value of n for 7 GHz becomes somewhat smaller than that one for 16 GHz ($n = 3.6$).

Test of Isotropy (Exp. C)

As mentioned in chap. 3 on certain assumptions experiment C) gives informations about the degree of isotropy of the turbulent refractive index field (or wind field). Fig. 9 shows the dependence of the mean receiving fieldstrength (with reference to the antenna orientation $\gamma = 0$, i. e. dir $\vec{K}$ is vertical) as a function of the azimuthal antenna orientation ($0° \leq \gamma \leq 45°$).

Only cases of vertical antenna elevations of $\alpha = 1°$ and $\alpha = 2°$ have been considered (in fig. 9) during two different propagation conditions ($z^* \leq 4$ m, fig. 9a, 7 m $\leq z^* \leq 8$ m, fig. 9b). Obviously, the observed increase of fieldstrength differences depends as well on frequency as on thickness of the evaporation duct. A considerable difference of fieldstrength between antenna elevations $\alpha = 1°$ and $\alpha = 2°$ only exists on 7 GHz, thus applying to the different propagation conditions, too. These results are probably caused by the fact that for 16 GHz the scattered field dominates in any case whilst this is valid for 7 GHz only in case of the collective "$\alpha \geq 2°$, $z^* \leq 4$ m". Therefore only the results of this set of data may be discussed (fig. 9c). On the frequency of 7 GHz a difference in fieldstrength of 7.6 dB between orientation $\gamma = 0°$ and $\gamma = 45°$ was observed; the corresponding value of 16 GHz was 3.1 dB. If we take into account the influence of height differences on the fieldstrength (experiment B) on 7 GHz (1.1 dB/100 m) the observed value reduces to 3.1 dB (fig. 9c). This

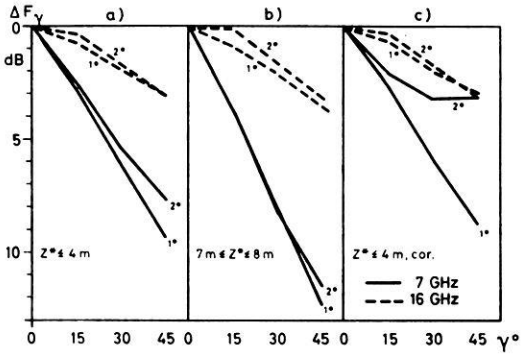

Fig. 9: Decrease of averaged fieldstrength as a function of azimuthal elevation angle γ for vertical antenna elevation $\alpha = 1°$ and $\alpha = 2°$. Left and central figure: non-corrected values for different intervals of thickness of evaporation duct. Right figure: values, corrected by the decrease in elevation.

means that for the orientation of $\gamma = 45°$ there is practically no difference between 7 and 16 GHz. The result of this experiment first involves the impression of anisotropy of the turbulent refractive index field because

$$\Phi(\vec{K})_{\text{dir } \vec{K}=0°} / \Phi(\vec{K})_{\text{dir } \vec{K}=45°} > 1 .$$

The consequence would be that $\vec{K}_{\gamma=0°} < \vec{K}_{\gamma=45°}$ and $L_{\gamma=0°} > L_{\gamma=45°}$ (equ. 3), i. e. the vertical extension of the scattering blobs is larger than the horizontal one. The inverse case

$$\Phi(\vec{K})_{\text{dir } \vec{K}=0°} / \Phi(\vec{K})_{\text{dir } \vec{K}=45°} < 1$$

was hardly ever observed ($\approx 3\%$ of all cases). The fieldstrength difference of 3 dB between orientation $\gamma = 0°$ and $\gamma = 45°$ corresponds to the ratio of $\Phi(\vec{K})_{\text{dir } \vec{K}=0°} / \Phi(\vec{K})_{\text{dir } \vec{K}=45°} = 1.15$. Provided that the assumption of chap. 2 is valid and supposing an exponent $n = 11/3$ of the refractive index spectrum one obtains the ratio $L_{0°}/L_{45°} = 1.03$. From this, however, one sees that the observed fieldstrength difference is too small to play any role for anisotropy. That means that in this case the turbulent refractive index field may be considered as an isotropic one, a fact which corresponds to the results of chap. 4.2.

4.4. *Atmospheric Effects on Signal Fading*

Fading Speed

Fig. 4a shows in the lower part the angular dependence of the fading rate. If the influence of the evaporation duct can be neglected the fading rate generally increases with the elevation angle according to the fading theory.

According to equ. (6) an interdependence between the fading rate and the cross-path component of wind speed is suggested. Fig. 10 shows the fading rate for elevation $\alpha = 0°$ and $\alpha = 2°$ as a function of cross-path (u_N) and parallel path component (u_T) of wind speed, both the components being derived from surface measurements on light house ship Elbe 1. (The correspondent correlation with the wind a higher levels changes the results not fundamentally as the further analysis yields). The linear dependence due to the fading theory of Rice [1954] can only be observed in the case of quasi-horizontal radiation. Regarding the observed values for elevation $\alpha = 2°$, one has to take into account a considerable deviation from the theory and a distinct non-linear correlation.

Cumulative Distributions of the Fading Amplitude

Cumulative distributions of the amplitudes of fading (fig. 11) were derived from samplings of 2-min-periods for different elevation angles and three different meteorological situations ($z^* \approx 0$ m; 6 m and 13 m). According to the theory of Rice distri-

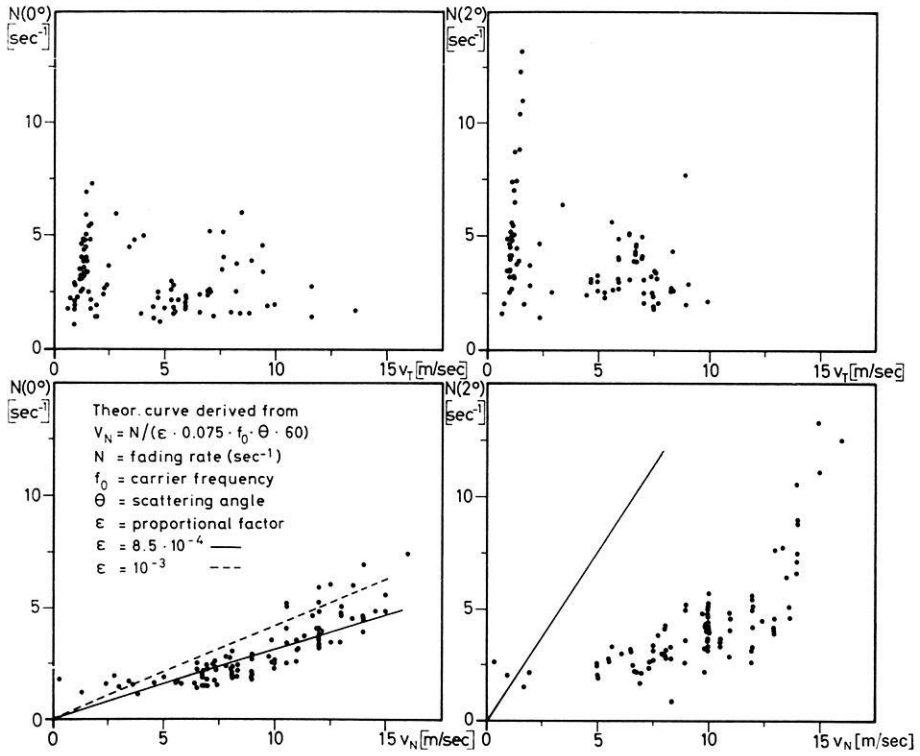

Fig. 10: Fading rate for antenna elevation angles $\alpha = 0°$ and $\alpha = 2°$ as a function of wind speed components normal (v_N) and parallel (v_T) to the propagation path.

bution (s. chap. 2.4.) even for more considerable antenna elevations more or less normal distributions are obtained in the case of well-marked evaporation ducts. During poor propagation conditions (vanishing duct) the observed distributions approach the Rayleigh distribution or the Rice distributions characterized by an increasing fluctuation (scatter) component.

The fading depth (10—90%-value) was derived from all cumulative distributions calculated. Fig. 12 shows the fading depth during different antenna elevations ($\alpha = 0°$, 1°, 2°) as a function of the median level of received fieldstrength during antenna elevation $\alpha = 0°$. A remarkably strong dependence of the fading depth on the receiving fieldstrength on the one hand, and on the antenna elevation on the other hand can be observed.

Considering the magnitude of observed fading depths and their relation to median fieldstrength, one should for a first approximation be able to evaluate the magnitude of the separated fields [NORTON et al., 1955]. The probability of a dominating scatter field during periods of $\alpha = 0°$-fieldstrength <25 dB, is even for 7 GHz, very high

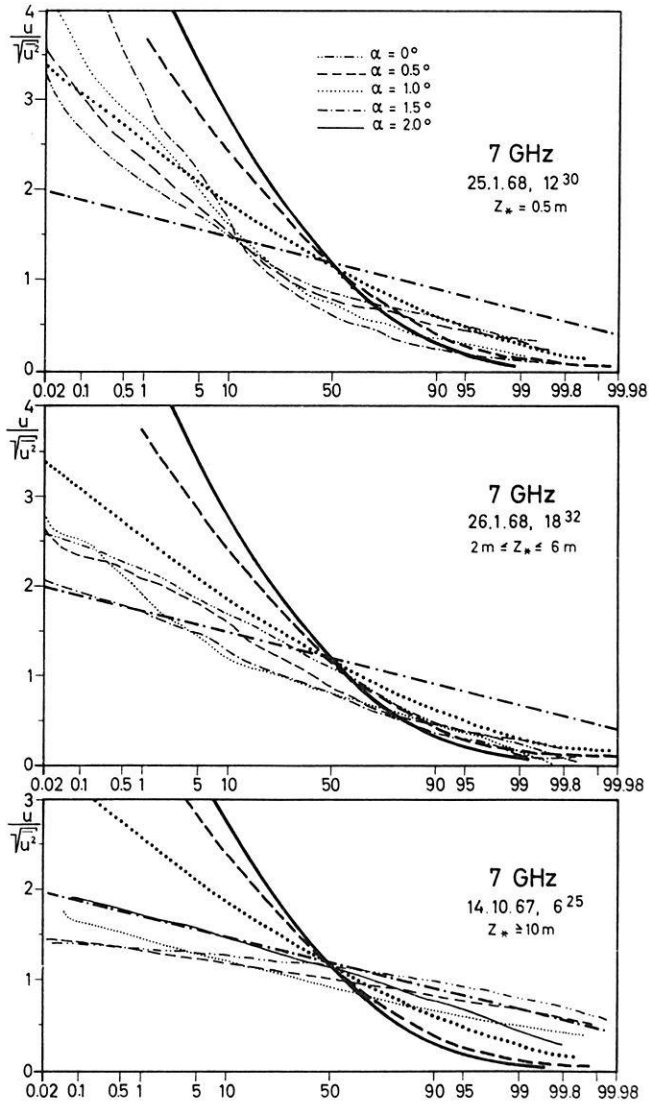

Fig. 11: Examples of cumulative distributions of the receiver signal voltage u ($\sqrt{\bar{u}^2}$ = rms-value);

——— Rayleigh, — — — $E_s/E_k = 3.2$, ····· $E_s/E_k = 1.0$, · — · — · $E_s/E_k = 0.32$; E_s/E_k = ratio of Rayleigh vector to constant vector.

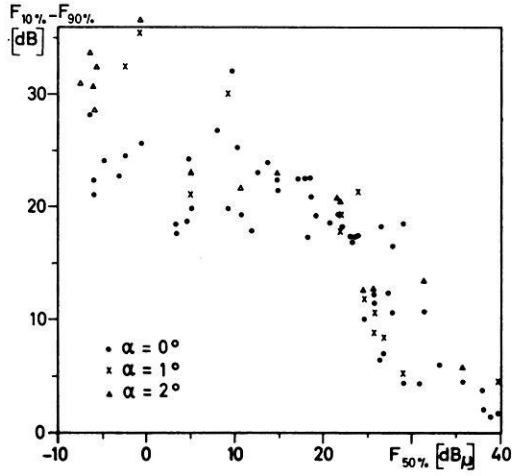

Fig. 12: Fading depth ($F_{10\%} - F_{90\%}$) for different antenna elevations as a function of median value ($F_{50\%}$) for antenna elevation $\alpha = 0°$.

because the fading depths in this case exceed 12 dB in magnitude. That is to say the scattering component exceeds the constant component of fieldstrength by more than 10 dB, i. e. the received field can be partically considered as a scatter field. Not to mention that this result proves to be valid for more considerable antenna elevations.

Generally, we may conclude that fading becomes the more intensive (larger fading depth, higher fading rate) the more the duct thickness decreases (corresponding to a low fieldstrength level) and the more the antenna elevation angle increases. Both facts point to an increase of the scattering component during poor propagation conditions.

5. Acknowledgement

The authors are very obliged to Prof. Dr. K. Brocks, director of the "Meteorologisches Institut der Universität Hamburg" and the "Institut für Radiometeorologie und Maritime Meteorologie an der Universität Hamburg" who encouraged this work in a generous way. They gratefully acknowledge the assistance of all colleagues who participated in the measurements and data processing. They also thank Dr. D. W. Thomson (University of Wisconsin, USA) for helpful discussions and critical comments during the preparation of the paper. For preparing the drawings Mrs. I. Voss was responsible.

The project was subsidized by the "Deutsche Forschungsgemeinschaft".

References

BIRKEMEIER, W. P., H. S. MERRILL, JR., D. H. SARGEANT, D. W. THOMSON, C. M. BEAMER, and G. T. BERGEMANN: Observation of Wind-produced Doppler Shifts in Tropospheric Scatter Propagation, Radio Science, 3 (New Series), No. 4, 309—317, 1968

BOOKER, H. G., and W. WALKINSHAW: The mode theory of tropospheric refraction and its relation to wave-guides and diffraction
In "Meteorological Factors in Radio Wave Propagation", published by the Physical Society and the Royal Meteorological Society, London, 80—127, 1946

BROCKS, K.: Der Brechungsindexgradient für elektromagnetische Wellen (Cm- bis M-Band) in der maritimen Grenzschicht der Atmosphäre, Dt. Hydrogr. Zeitschr., 8, 186—194, 1953

CRAWFORD, A. B., A. B. HOGG, and W. H. KUMMER: Studies in tropospheric Propagation beyond the horizon, Bell Syst. Tech. J. 38, No. 5, 1068—78, 1959

DU CASTEL, F., J. VOGE, A. SPIZZICHINO, and P. MISME: Propagation Troposphérique et Faisceaux Hertziens Transhorizon Télécommunication par Satellites, Editions Chirons, 40, rue de Seine, Paris, 1960

EKLUND, F.: The Wavelength Dependence of Tropospheric Beyond-the-Horizon Propagation, AGARD (NATO) Conference Proceedings No. 37, Scatter Propagation of Radio Waves, Part 1, 19, 1968

FRIIS, H. T., A. B. CRAWFORD, D. C. HOGG: A Reflection Theory for Propagation Beyond the Horizon, Bell Syst. Tech. J., 36, No. 5, 627—644, 1957

GJESSING, D. T.: Determination of Permittivity Variations in the Troposphere by Scatter-Propagation Methods, Proc. IEE, Part C, 109, 447—455, 1962

GJESSING, D., H. JESKE, and N. KLINT-HANSEN: An Investigation of the Tropospheric Fine Scale Proporties Using Radio, Radar and Direct Methods, J. Atm. Terrestr. Phys., 31, 1157—1182, 1969

GOSSARD, E. E.: Spectra of atmospheric scalars, J. Geophys. Res., 64, 2226—2229, 1960

JESKE, H.: Die Ausbreitung elektromagnetischer Wellen im cm- bis m-Band über dem Meer unter besonderer Berücksichtigung der meteorologischen Bedingungen in der maritimen Grenzschicht, Hamburger Geophysikalische Einzelschriften, Heft 6, Cram, de Gruyter u. Co., Hamburg 1965

JESKE, H., and K. BROCKS: Comparison of Experiments on Duct Propagation Above the Sea With the Mode Theory of Booker and Walkinshaw, Radio Science, 1 (New Series), No. 8, 891—895, 1966

KOONO, T., M. HIRAI, R. INOUE, and Y. ISHIZAWA: Antenna beam deflection loss and signal amplitude correlation in angle-diversity reception in UHF beyond-horizon communications, J. Radio Res. Labs. (Japan) 9, No. 41, 21—49, 1962

MEGAW, E. C. S.: Scattering of Electromagnetic Waves by Atmospheric Turbulence, Native, 166, No. 12, 1100, 1950

NORTON, K. A., L. E. VOGLER, W. V. MANSFIELD, and P. J. SHORT: The Probability Distribution of the Amplitude of a Constant Vector Plus a Rayleigh-Distributed Vector, Proc. IRE, 43, No. 10, 1354—1361, 1955

RICE, S. O.: Statistical fluctuations of radio field strength far beyond the horizon, Proc IRE, 41, No. 2, 274—281, 1953

TATARSKI, V. I.: Wave Propagation in a Turbulent Medium, McGraw-Hill Book Comp., Inc., New York, N. Y. 1961

VILLARS, F., and V. F. WEISSKOPF: The Scattering of Electromagnetic Waves by Turbulent Atmospheric Fluctuations, Phys. Rev. 94, 232—240, 1954

VILLARS, F., and V. F. WEISSKOPF: On the Scattering of Radio Waves by Turbulent Fluctuations of the Atmosphere, Proc. IRE, 43, No. 10, 1232—1239, 1955